

Review

Mitochondrial Dysfunction Induced by Zinc Oxide Nanoparticles

Leslie Patrón-Romero^{1,2}, Priscy Alfredo Luque-Morales^{2,*}, Verónica Loera-Castañeda³, Ismael Lares-Asseff³, María Ángeles Leal-Ávila⁴, Jorge Arturo Alvelais-Palacios⁵, Ismael Plasencia-López^{6,7} and Horacio Almanza-Reyes^{1,7,*} 

- ¹ Faculty of Medicine and Psychology, Autonomous University of Baja California, Tijuana 22390, Baja California, Mexico
- ² Faculty of Engineering, Architecture and Design, Autonomous University of Baja California, Ensenada 22860, Baja California, Mexico
- ³ Instituto Politécnico Nacional, CIIDIR-Unidad Durango, Durango 34220, Durango, Mexico
- ⁴ University Center for Health Education, Autonomous University of Baja California, Tijuana 22010, Baja California, Mexico
- ⁵ School of Health Sciences, Valle de Las Palmas, Autonomous University of Baja California, Tijuana 22260, Baja California, Mexico
- ⁶ Faculty of Accounting and Administration, Autonomous University of Baja California, Tijuana 22390, Baja California, Mexico
- ⁷ Bioeconomy Cluster of Baja California, A.C., Tijuana 22040, Baja California, Mexico
- * Correspondence: pluque@uabc.edu.mx (P.A.L.-M.); almanzareyes@uabc.edu.mx (H.A.-R.)



Citation: Patrón-Romero, L.; Luque-Morales, P.A.; Loera-Castañeda, V.; Lares-Asseff, I.; Leal-Ávila, M.Á.; Alvelais-Palacios, J.A.; Plasencia-López, I.; Almanza-Reyes, H. Mitochondrial Dysfunction Induced by Zinc Oxide Nanoparticles. *Crystals* **2022**, *12*, 1089. <https://doi.org/10.3390/cryst12081089>

Academic Editors: Yamin Leprince-Wang, Guangyin Jing and Basma El Zein

Received: 1 July 2022

Accepted: 26 July 2022

Published: 4 August 2022

Publisher's Note: MDPI stays neutral with regard to jurisdictional claims in published maps and institutional affiliations.



Copyright: © 2022 by the authors. Licensee MDPI, Basel, Switzerland. This article is an open access article distributed under the terms and conditions of the Creative Commons Attribution (CC BY) license (<https://creativecommons.org/licenses/by/4.0/>).

Abstract: The constant evolution and applications of metallic nanoparticles (NPs) make living organisms more susceptible to being exposed to them. Among the most used are zinc oxide nanoparticles (ZnO-NPs). Therefore, understanding the molecular effects of ZnO-NPs in biological systems is extremely important. This review compiles the main mechanisms that induce cell toxicity by exposure to ZnO-NPs and reported in vitro research models, with special attention to mitochondrial damage. Scientific evidence indicates that in vitro ZnO-NPs have a cytotoxic effect that depends on the size, shape and method of synthesis of ZnO-NPs, as well as the function of the cells to which they are exposed. ZnO-NPs come into contact with the extracellular region, leading to an increase in intracellular [Zn²⁺] levels. The mechanism by which intracellular ZnO-NPs come into contact with organelles such as mitochondria is still unclear. The mitochondrion is a unique organelle considered the “power station” in the cells, participates in numerous cellular processes, such as cell survival/death, multiple biochemical and metabolic processes, and holds genetic material. ZnO-NPs increase intracellular levels of reactive oxygen species (ROS) and, in particular, superoxide levels; they also decrease mitochondrial membrane potential (MMP), which affects membrane permeability and leads to cell death. ZnO-NPs also induced cell death through caspases, which involve the intrinsic apoptotic pathway. The expression of pro-apoptotic genes after exposure to ZnO-NPs can be affected by multiple factors, including the size and morphology of the NPs, the type of cell exposed (healthy or tumor), stage of development (embryonic or differentiated), energy demand, exposure time and, no less relevant, the dose. To prevent the release of pro-apoptotic proteins, the damaged mitochondrion is eliminated by mitophagy. To replace those mitochondria that underwent mitophagy, the processes of mitochondrial biogenesis ensure the maintenance of adequate levels of ATP and cellular homeostasis.

Keywords: mitochondria; apoptosis; zinc oxide; nanoparticles

1. Introduction

The almost universal applications of metallic nanoparticles (NP) in daily life increase the probability of being in constant contact with them; therefore, investigating the beneficial and harmful effects is of particular relevance. Due to their multiple areas of application, among the most relevant NPs are zinc oxide NPs (ZnO-NPs). Its usefulness in the biomedical field is undoubtedly among the most relevant and promising advances. Within the

nanotechnology industry, it is among the most synthesized NPs, ranking below silver and gold NPs [1,2]. Even though ZnO-NPs offer essential benefits in many areas, such as the pharmacological, medical, biochemical, and microbiological, some studies show that ZnO-NPs can cause harmful effects compared to other metallic NPs such as Fe₃O₄, Al₂O₃, and TiO₂ [3–6]. Unlike their therapeutic applications in the oncology field, toxicological studies have shown that ZnO-NPs can represent a severe danger to specific tissues and organs, such as the lungs, skin, or muscles, to name a few [6–8]. Therefore, investigating the potential health risk due to increased exposure has recently generated concern. ZnO-NPs can enter indirectly through contact or consumption of previously exposed water, plants, and animals, or they can enter directly through inhalation, dermal contact, ingestion, or absorption.

ZnO-NP morphology depends on the synthesis process. They may be nanospheres, nanoplates, nanowires, nanotubes, nanorings, nanocages, nanoflowers, nanoflakes, or hexagonal. ZnO-NPs penetrate the cell membrane by multiple mechanisms, the most studied are ion channels (located both in the cell membrane and in the mitochondrial membrane), specific receptors for metal ions, endocytosis and by direct uptake of ZnO-NPs. Size and shape play a crucial role. The smaller the ZnO-NPs, the more easily they enter the cells and the greater the cytotoxic effect (<50 nm), due to the higher surface area/volume ratio. Morphology plays another relevant role—for example, spherical and hexagonal shapes penetrate easier than tubular shapes. In terms of surface charge, positively charged ZnO showed high cellular uptake compared to ZnO with negative charge. Additionally, the toxicity of nanoparticles, releasing toxic ions, has been considered. Since zinc oxide is amphoteric in nature, it reacts with both acids and alkalis, giving Zn²⁺ ions.

Once ZnO-NPs are internalized in the cell, they are distributed in all the organelles, particularly in the mitochondria [9,10]. The mitochondria is a unique organelle considered the “energy supply center” of the cell, present in all eukaryotic organisms and all mammalian cells. Mitochondria are responsible for numerous cellular processes, such as β-oxidation of fatty acids, amino acid metabolism, pyridine synthesis, phospholipid modifications, generation of reactive oxygen species (ROS), oxidative stress homeostasis, cell death/survival, and senescence. It is also well known that, in multicellular organisms, the number of mitochondria is variable. The number of mitochondria will depend on energy demands, function, and stage of development [11].

At the structural level, mitochondria are composed of an outer membrane and an inner membrane; the latter contains proteins involved in the electron transfer chain (ETC). The integrity of the ETC is crucial for ATP generation; as a result of its activation, reactive oxygen species (ROS) are generated. ROS are responsible for causing cellular stress, mutations and induce apoptosis [4]. The mitochondria carries a unique genetic material, which is characterized by having a circular double-strand (without ends) of nucleic acids called mitochondrial DNA (mtDNA), containing information to encode 37 genes—of which 13 genes encode for messenger RNA (mRNA), from which 13 mitochondrial proteins are subsequently obtained. Two genes encode ribosomal RNA (rRNA), and 22 genes synthesize transference RNA (tRNA). This smaller but no less critical genome is replicated, transcribed, and translated within the mitochondrial matrix, independently of cell cycle phases. Like nuclear genetic material, mtDNA is susceptible to genotoxicity produced by chemical (ZnO-NPs) and physical agents [12]. This review compiles the most relevant mechanisms leading to mitochondrial dysfunction caused by ZnO-NP exposure.

This review compiles the multiple mitochondrial pathways affected by toxicity after exposure to ZnO-NPs, among which loss of mitochondrial membrane potential, depletion of ATP synthesis due to electron transport chain abnormality, mtDNA synthesis, mitochondrial biogenesis, cell survival and apoptosis are mentioned in detail. The cytotoxicity induced by ZnO-NPs depends on numerous factors, such as ZnO-NPs synthesis methodology, nanoparticle size, morphology, concentration, exposure time and, not least, the type of cell exposed. Factors associated with cellular response include the stage of differentiation, e.g., a differentiated cell versus a cell of embryonic origin and whether the cell is healthy or

tumorigenic. In the case of differentiated human cells, liver, neuronal, cardiac, epidermal, fibroblast, blood and other cells were included; and for tumor models: hepatocyte cancer cell, breast cancer, multiple myeloma cell, cervical cancer, etc. The maximum inhibitory concentration (IC₅₀) and biological methods to obtain it were investigated. Finally, a concise discussion was made on the most relevant factors involved in the mitochondrial and cellular response after exposure to ZnO-NPs found in the most updated literature.

ZnO-NPs penetrate the cell membrane via four mechanisms: the first mechanism involves receptors associated with effector proteins that activate multiple signaling pathways. In the second mechanism, ion channels located in the mitochondrial membrane and cell membrane facilitate entry into the cytoplasm. The third mechanism is endocytosis—in this process, a fragment of the lipid cell membrane covers ZnO-NPs, allowing the formation of vacuoles, which later merge with the membranes of other organelles such as the nucleus and the mitochondria. The fourth mechanism is direct absorption, in which ZnO-NPs (depending on their size and shape) penetrate the cellular lipid bilayer. The entry of ZnO-NPs is also facilitated by two specialized zinc transporters—ZnT1 and ZnT2. Zinc dissociation also occurs, and zinc can penetrate as zinc ions.

2. Impairment of Mitochondrial Biogenesis Induced by ZnO-NPs

Mitochondrial biogenesis is essential to maintain the proper mitochondrial population and cellular functioning. In humans, it is estimated that >50% of the cytoplasm volume is occupied by the mitochondrial mass, >30% in cardiomyocytes and >25% in fibroblasts [13]. Under physiological conditions, the induction of mitochondrial biogenesis is associated with the activation of transcription factors that act on nuclear DNA (nDNA) and mtDNA to control local (within mitochondria) or cytoplasmic protein synthesis [14]. For example, exercise increases mitochondrial protein synthesis, resulting in mitochondrial biogenesis in skeletal muscles [15]. The half-life of mitochondria depends on multiple factors, such as ATP demand and cellular function. Severely damaged mitochondria will be eliminated by mitophagy to prevent the release of pro-apoptotic proteins. The fine coordination between these two opposing processes will determine mitochondrial homeostasis [16,17]. Some of the factors involved in mitochondrial biogenesis are mitochondrial fission protein 1 (FIS1) and mitochondrial fission factor (MFF), which promote mitochondrial fission by recruiting GTPase dynamin-related protein 1 (DRP1) [18,19].

Other factors involved in regulating mitochondrial biogenesis include mitochondrial transcription factor A (mtTFA), which drives mtDNA transcription and replication. The expression of mtTFA is regulated by the peroxisome proliferator-activated receptor gamma-coactivator 1 α (PGC-1 α) and PGC-1 β , which are the main regulatory proteins of mitochondrial biogenesis [20]. More recently, the involvement of NF-E2-p45-related factor 2 (NRF2), encoded by the NFE2L2 gene, has gained attention. Free NRF2 translocates to the nucleus, where it targets the promoters of genes that induce mitochondrial biogenesis [21]. Li et al., [22] in 2013, reported the adverse effects caused in mature human cardiomyocytes derived from human stem cells after exposure to ZnO-NPs. They proposed that ZnO-NPs could alter mitochondrial biogenesis, as shown by decreased mitochondrial density, altered mtDNA copy number, and inhibition of the PGC-1 α pathway that eventually lead to mitochondrial depletion. The mtDNA replication and transcription system is activated to counteract oxidative damage inflicted on the mitochondrial respiratory chain under mild oxidative stress. When cellular stress increases, mitochondrial biogenesis intervenes to maintain cellular homeostasis.

Yousef et al., [23] reported similar results in 2019, where they performed a quantitative analysis of mtTFA and PGC-1 α expression in rat-derived liver and kidney cells. The results showed significant suppression of hepatic mtTFA expression by approximately 62% relative to the control value and, similarly, suppression in PGC-1 α expression by approximately 51% relative to the control group, following ZnO-NP exposure. In addition, increased expression of the tumor suppressor gene p53, which is involved in the induction of apoptosis, was documented. On the other hand, mitochondria are highly dynamic

organelles, constantly undergoing fission and fusion processes in response to changing energy demands and cellular stress environments. Mitochondrial fusion is mediated by proteins such as mitofusin 1 (MFN1) and mitofusin 2 (MFN2), located on the outer mitochondrial membrane [24]. Phosphatidylserine decarboxylase (PSD1), located in the inner mitochondrial membrane, is involved in the biosynthesis of phosphatidylcholine, which in turn regulates mitochondrial fusion. Another protein involved is optic atrophy 1 (OPA1), which participates in the inner membrane fusion and apoptosis [25,26].

In 2018, Babele et al., [27] reported that exposure to ZnO-NPs conditioned the release of mitochondrial PSD1 into the cytosol. This indicated loss of integrity in the inner mitochondrial membrane, decreased levels in biogenesis, and defects in lipid metabolism. A year later, to expand on the toxic effects of ZnO-NPs, Babele et al. combined a proteome and metabolome analysis. He identified 46 metabolites (including seven unknown). Among those affecting the oxidative pathway were Super Oxide Dismutase 1 (SOD1), Super Oxide Dismutase 2 (SOD2), and yeast AP-1 (YAP1). The metabolites involved in lipid biosynthetic pathways were transcription factor 2 requiring INOsitol (INO2), transcription factor 4 requiring INOsitol (INO4), CHoline requiring CHO1, cardiolipin synthase (CRD1), and PSD1. The aforementioned metabolites are involved in crucial mitochondrial processes, i.e., glycolysis, the tricarboxylic acid cycle (TCA), pentose phosphate pathway, and central carbon metabolism (CCM) in the *Saccharomyces cerevisiae* model [28]. Up to 10% of the proteins encoded by the human genome interact with zinc ions. Approximately 3000 proteins interact with zinc ions, acting mainly as a cofactor [29]. Therefore, determining how ZnO-NP are internalized, transported, and distributed within the cell and mitochondria is of particular interest. Zinc transporter 2 (ZnT2) was the first zinc transporter found. In 2020, Chevallet et al., [30] reported a 30- to 40-fold dose-dependent overexpression of ZnT2 in human hepatocytes (HepG2) with a dose-dependent effect. This proposed active sequestration of ZnO-NPs into mitochondria by ZnT2. Abnormalities in mitochondrial morphology were also reported, suggesting disruptions in mitochondrial fission and fusion dynamics after exposure to ZnO-NPs. Skin cells are among the most exposed tissues due to the use of sunscreens and beauty products. In 2013, Yu et al. showed in normal mouse-derived skin the alteration of mitochondria; ZnO-NP exposure negatively affects mitochondrial network and biogenesis after 48 h of exposure [31]. In 2020, Khan et al. proposed that dose-dependent abnormalities in mitochondrial morphology and a significant increase in apoptotic behavior in human skin carcinoma A431 cells compared to normal renal epithelial NRK-52E cells may be due to a higher expression of anionic membrane phospholipids in cancer cells [32]. Table 1, presents numerous cytotoxicity studies in various biological systems, both in embryonic cell lines and in differentiated human and non-human cells, healthy and tumor cells, exposed to ZnO-NPs. Morphological characteristics are described, as well as dose, time and molecular analysis, to facilitate comparative analysis.

Figure 1, shows a compilation of the main molecular pathways involved by exposure to ZnO-NPs, including their entry into the membrane, effect on the cell nucleus, mitochondria and, finally, activation of apoptosis.

Table 1. Cell models exposed to dose-time-dependent ZnO-NPs and the mitochondrial pathway analyzed.

Cell Type	Size and Shape of ZnO-NP	Synthesis and Characterization of ZnO-NPs	Time of Exposition (h)	Doses mg/L	IC50	Biological Characterization	Mitochondrial Pathway	Reference
Human embryonic kidney cells (HEK293T) Chicken embryo (cranial neural crest cells HH10)	<50 nm Spherical shape	Synthesis method ND/OC. TEM, SEM-EDS, DLS	12 h	12.5, 25, 50, 100, 200 µg/mL	50 µg/mL ND *	Cell culture, CCK-8, CNCCs, ARS, IHC, RNA-seq, q-PCR, DAPI, FM/IFA	Ion release triggered ROS production, which further induced cell toxicity, inflammation and apoptosis, which are mediated by NF-κB signaling cascades and mitochondria dysfunction. Increase in the expression of Nrf2, HO-1, NQO1, Cat, GLXR and NOS. Increase in Pax7 and Casp-3 expression.	[8]
Human cardiomyocytes (hiPSC-CMs)	40 nm–60 nm Spheroid and rod shaped	Synthesis method ND/OC. TEM, DLS	0, 2, 6 h	0–200 µg/mL	62.5 µg/mL	Cell culture, LDH, HCA, CCK-8, MMP, ROS, q-PCR, WB, MEA	ROS generation and induced mitochondrial dysfunction. Impair mitochondrial biogenesis and inhibit the PGC-1α pathway. Cardiac electrophysiological alterations.	[22]
Human epidermoid carcinoma cell A431 Normal kidney epithelial NRK-52E cells	<40 nm Hexagonal structure	Chemical synthesis by reduction Zinc acetate dyhydrate XRD, TEM, SEM, UV-Vis	24 h 24 h	0–25 µg/mL	24 µg/mL 15 µg/mL NS *	Cell culture, MTT, FM, ROS, DAPI, Casp-3 and cell morphology	The anti-proliferative activity, morphological changes, ROS generation, nuclear apoptosis and caspase-3 in a dose-dependent manner.	[32]
Human aortic endothelial cells (HAECs)	70 nm Rod shaped	Synthesis method ND/OC. TEM, XRD	12 or 24 h	8–50 µg/mL	50 µg/mL	Cell culture, MTT, LDH, ROS, FM, MMP, LA, CACAK, Cas-3, Cas-9, Cyt-c, ICC, IFA	Apoptosis was confirmed using reactive oxygen species (ROS). Decrease in MMP. Increased release of Cyt-c. Caspase-3, caspase-9, BAX, BCL-2 and FAS receptor expression. The antioxidant LA was able to protect HAECs from apoptosis induced by ZnO-NPs.	[33]
Human tenon fibroblast (HTF)	56 nm ND	Synthesis method ND/OC. TEM	24 h 48 h 72 h	0–16.0 µg/mL	1.51 µg/mL 1.03 µg/mL 0.57 µg/mL	Cell culture, CCK-8, RT-CES, ROS, FM, MMP, qPCR, FC, Apaf-1, Cas-3, Cas-9, FSP-1	Inhibit the viability of HTFs and decrease MMP. Elevated ROS, caspase-3, caspase-9, and apoptotic Apaf-1 expression. Decrease the levels of FSP-1, collagen III, and E-cadherin expression, leading to HTF apoptosis.	[34]
Human erythrocytes	47.8–52.5 nm Rod shaped	Chemical synthesis by Pechini method XRD, TEM, FTIR	1 h	50–500 µg/mL	200 µg/mL	Cell culture, H, SOD, CAT, LPO, GST, GSH, ROS, OH, O2, CA, IFA/FM	Concentration-dependent hemolytic activity to human erythrocytes. ROS generation. Depletion of glutathione and GST levels. Increased SOD, CAT and lipid peroxidation in dose-dependent manner.	[35]

Table 1. Cont.

Cell Type	Size and Shape of ZnO-NP	Synthesis and Characterization of ZnO-NPs	Time of Exposition (h)	Doses mg/L	IC50	Biological Characterization	Mitochondrial Pathway	Reference
Human monocytes U-937 Human promyelocytes HL-60 Human B lymphocytes COLO-720L Human T lymphocytes HUT-78	15 nm ND	Synthesis method ND/OC. TEM, DLS	24 h	1.6–25 µg/mL	1.5625 µg/mL 3.125 µg/mL 6.25 µg/mL 12.5 µg/mL 25 µg/mL	Cell culture, MTT, LDH, MDA	ZnO-NPs caused lipid peroxidation of all cells and correlated with apoptosis. The level of cholesterol in membranes strongly modifies the effect exerted by ZnO-NPs.	[36]
Human monocytes U-937 Human promyelocytes HL-60 Human B lymphocytes COLO-720L Human T lymphocytes HUT-78	100–130 nm ND	Synthesis method ND/OC. TEM	24 h	0–25 µg/mL	1.56 µg/mL 3.12 µg/mL 6.25 µg/mL 12.5 µg/mL 25 µg/mL	Cell culture, MTT, LDH, NO, MDA, Casp-9, IL-6, TNF-α	Activation of the mitochondrial apoptosis pathway. TNF-α concentration increased for both cell lines. IL-6 concentration rose on average 5-fold in HL-60 cells in all experimental variants, the opposite trend was observed for COLO-720L. ZnO-NPs are cytotoxic to immune system and cause peroxidation of membrane lipids.	[37]
Human colon carcinoma (HCT116) Human myelogenous leukemic (K562)	30–48.5 nm Hexagonal structure	Green Synthesis method (<i>Spondias pinnata</i>) UV-Vis, FTIR, XRD, FESEM, HRTEM, EDX	24 and 48 h	0.25–200 µg/mL	82 and 60 µg/mL 55 and 35 µg/mL	Cell culture, MTT, IFA/FM, VWH, MMP, FC, CA, DNaf, RT-qPCR, WB, H	Upregulation of pro-apoptotic (PUMA, Bax, Cyt-c, cas-9, cas-3, and PARP) and downregulation of anti-apoptotic (Bcl-2 and survivin) genes. Elevation in the expression of Cyt-c, cas-9, and cas-3 genes involved in mitochondrial (intrinsic) apoptotic pathway.	[38]
Human keratinocytes (HaCaT) Human gingival fibroblast (HGF-1) Human gingival carcinomas (Ca9-22) Human gingival carcinomas (OECM-1)	100 nm ND	Synthesis method ND/OC. SEM	24 h	0–100 µg/mL	100 µg/mL 100 µg/mL 17.4 ± 0.6 µg/mL 51.0 ± 0.6 µg/mL	Cell culture, MTT, ROS, MMP, WB, ZXA, FC	Mitochondrial oxidative damage and p70S6K signaling pathway inhibition, caspase-3, caspase-8, caspase-9 and PARP activation. Induce sub-G1 arrest of the cell cycle followed by apoptosis in human GSCC. ROS is essential for the anti-cancer activity. Did not affect the expression of pro-survival Bcl-2 members (Bcl-2, Bcl-xl, and Mcl-1) as well as pro-apoptosis Bcl-2 members (Bax, Bad, and Bid).	[39]
Human oral cancer (CAL 27)	50 nm Hexagonal prism	Synthesis method ND/OC. TEM, XRD and DLS	24 h	0–100 µg/mL	25 µg/mL	Cell culture, CCK-8, LC3, P62, GAPDH, PINK1, Parkin, IHC, ROS, MDC, MMP, WB, JC-I, ROS	Increased ROS levels, decreased MMP and mitochondrial dysfunction time-dependent manner. Increased levels of LC3-II, PINK1, mito-Parkin and decreased P62 and Parkin.	[40]

Table 1. Cont.

Cell Type	Size and Shape of ZnO-NP	Synthesis and Characterization of ZnO-NPs	Time of Exposition (h)	Doses mg/L	IC50	Biological Characterization	Mitochondrial Pathway	Reference
Human hepatocytes (HepG2)	237 nm 79 nm Rod shaped and spherical	Synthesis method ND/OC. TEM, ICP-AES, EDX and DLS	24 h	0–300 µg/mL	>150 µg/mL	Cell culture, qRT-PCR, AVO, MMP, TBEA, SOD, CAT	Increased mitochondrial zinc transporter 1 and 2 expression levels. Response and the upregulation of MET, ZnT1, ZnT2, no change in CAT, SOD1 and SOD2 expression, nor in the enzymatic activities of catalase and SOD, implying a minimal activation of oxidative stress. Abnormal mitochondria morphologies and autophagy vesicles in response to ZnO-NPs.	[30]
Human hepatocytes (HL-7702) Human colorectal (Caco-2)	<100 nm ND	Synthesis method ND/OC. ICP-MS, TEM, SEM	3 h	0.665 µg/mL	NS * NS *	Cell culture, MTT, LDH, MMP, ROS, qRT-PCR	Increased ROS levels due to NP exposure, overexpression of HMOX1 in response to the increased oxidative stress. The cytotoxicity induced by high ROS levels, oxidative stress and depolarization of mitochondrial membrane.	[41]
Huh7 hepatocytes cancer cell line	18 nm Polycrystalline nature	Green synthesis (<i>Luffa acutangula</i>) UV-Vis, HRTEM, SAED	8 h	0–60 µg/mL	40 µg/mL	Cell culture, MTT, ROS, MMP, DNAf. FM	Huh 7 liver cancer cells undergo apoptosis as a result of generation of ROS molecules. Stimulation of apoptotic signaling pathway in a dose-dependent manner. Condensed chromatin and fragmented DNA.	[42]
Human hepatocytes (HepG2) Human breast cancer (MCF-7)	~13 ± 2 nm ND	Chemical synthesis by reduction Zinc acetate dihydrate FESEM, TEM, XRD, FTIR, UV-Vis	24 and 48 h	0–100 µg/mL	25 and 10 µg/mL 25 µg/mL	FC, MTT, FACS, qRT-PCR, cell morphology, Casp-3, p53, Bax, Bcl-2	Significant upregulation of mRNA expression levels of Bax, p53, and caspase-3 and the downregulation of the anti-apoptotic gene Bcl-2.	[43]
Human breast cancer (MCF-7)	41 nm flakes Hexagonal	Chemical synthesis Triethanolamine XRD, FESEM, EDS	24 h	1–5 µg/mL	3 µg/mL	Cell culture, MTT, DPPH, AO/EB, PI	Dose-dependent loss of cell viability. ZnO-NP exposure increases necrosis and apoptosis of MCF cells.	[44]
Human breast cancer (MCF-7)	43 nm Spherical	Synthesis using sol-gel method. XRD, HR-TEM, EDS, TEM, XRD	24 h	0–100 µg/mL	44 µg/mL	Cell culture, MTT, LDH, ROS, GSH, TSH, MMP, IFA/FM, q-PCR	Upregulation of apoptotic genes (p53, Bax/Bcl2 ratio, caspase-3 and caspase-9). Loss of MMP and apoptosis in MCF-7 cells through the mitochondrial pathway.	[45]

Table 1. Cont.

Cell Type	Size and Shape of ZnO-NP	Synthesis and Characterization of ZnO-NPs	Time of Exposition (h)	Doses mg/L	IC50	Biological Characterization	Mitochondrial Pathway	Reference
Human breast cancer (MCF-7) Human Non-tumorigenic human mammary epithelial cell line (MCF-10A)	63.7 ±6.5 nm Spherical	Synthesis method ND/OC. DLS, AFM	24 and 48 h	0.5–20 µg/mL	20 and 10 µg/mL >90% IC50 with max doses	MTT, DAPI, qRT-PCR, IFA/FM and cell morphology	The increased expression of Bax/Bcl-2 ratio confirmed the induction of apoptosis in MCF-7 cells. ZnO-NPs induced casp3- and casp-8 upregulation.	[46]
Human multiple myeloma cell (RPMI8226) Peripheral blood mononuclear cell	30 nm	Synthesis method ND/OC. TEM	24 and 48 h	0–60 µg/mL	34 and 29 µg/mL 120 and 79 µg/mL	ROS, FC, q-PCR, ATP assay, cell morphology	Increase expression and proteins levels of caspase-3, caspase-9, Apaf-1, and Cyt-c, decrease ATP levels in time- and dose-dependent manner, ROS generation.	[47]
Human cervical cancer cell (SiHa)	20–50 nm	Green synthesis (<i>Gracilaria edulis</i>) UV-Vis, FTIR, XRD, FESEM, XPS, SEM, EDS, EDX and HRTEM	24 h	0–200 µg/mL	35 µg/mL	MTT, FC, ROS, MMP AO/EB, IFA/FM, CA, JC-I	Apoptotic and necrotic effect. ROS elevation, DNA damage, activation of mitochondrial intrinsic pathway.	[48]
Human cervical cancer cell line (HeLa)	10–70 nm	Green synthesis (<i>Aspergillus terreus</i>) UV-Vis, XRD, EDX, FTIR and TEM.	24 h	5–80 µg/mL	20 µg/mL	MTT, WB, SOD, CAT, ROS, MMP, p53, BAX, casp-3, casp-9, Cyt-c. Cell morphology.	Reduced SOD, CAT and GPO, increased ROS, diminished MMP. Upregulation of p53, casp-9, BAX, RAD51 and downregulation of BCL-2.	[49]
Human cervical cancer (HeLa) Human colon cancer (HT-29)	30 nm	Green synthesis (<i>Bergenia ciliata</i>) UV-Vis, FTIR, DLS, EDX, XDR and SEM	24 h	25–200 µg/mL	101.7 µg/mL 124.3 µg/mL	MTT, DPPH and ABTS assay	Increased ROS and cytotoxicity against cancer cells.	[50]
Human ovarian cancer (SKOV3)	20 nm	Synthesis method ND/OC. UV-Vis, TEM, XRD, FTIR and AFM	24 h	0–30 µg/mL	20–30 µg/mL	Cell morphology, MTT, ICC, JC-I assay, TUNEL, WB, ROS levels and IFA/FM	Genotoxicity, double DNA strand breaks and apoptosis. Loss of MMP, ROS increased levels. Upregulation of p53, casp-9, BAX, RAD51 and downregulation of BCL-2.	[51]
AGS gastric cancer cells	100 nm	Green synthesis (<i>Morus nigra</i>) UV-Vis, TEM, SEM, FT-IR, EDX and XDR	24 h	0–25 µg/mL	10 µg/mL	MTT, MMP, AO/EB, ROS, FC, CAT, TBARS, GSH SOD, RT-PCR	MMP decreased. Apoptosis induced by ROS generation and gene expressions of apoptosis markers effects, increased lipid peroxidation, cell cycle arrest.	[52]
Human osteosarcoma cell line (MG-63)	10–12 nm	Green synthesis (<i>Radix Rehmanniae</i>) UV-Vis, TEM, XRD and FTIR	24 h	5–80 µg/mL	30 µg/mL	MTT, MMP, WB. ROS, BAX, casp-3 and casp-9 levels. Morphology assay AO/EB	Increased levels of BAX, casp-3, casp-9. MMP decreased and ROS generation.	[53]

Table 1. Cont.

Cell Type	Size and Shape of ZnO-NP	Synthesis and Characterization of ZnO-NPs	Time of Exposition (h)	Doses mg/L	IC50	Biological Characterization	Mitochondrial Pathway	Reference
Human lymphocytes Mouse fibroblast cell (C2C12) Mouse myoblast cell (L929)	16–24 nm	Green synthesis (<i>Beta vulgaris</i>) HRTEM, FTIR, XRD	24 and 48 h	1×10^{-6} 100 $\mu\text{g}/\text{mL}$	37 and 30 $\mu\text{g}/\text{mL}$ 32 and 23 $\mu\text{g}/\text{mL}$ 28 and 20 $\mu\text{g}/\text{mL}$	MTT, TBEA, cell kinetic and morphology assay	Abnormal cell morphology, adherence and viability manner. Mitochondrial function. Increased doses-dependent mortality rate.	[54]
Mouse macrophage line (J774A1)	140 ± 16 nm	Synthesis method ND/OC. TEM, SEM DLS	24 h	200 $\mu\text{g}/\text{mL}$	8 $\mu\text{g}/\text{mL}$	IFA/FM, MMP, GAPDH assay, mass spectrometry, HPLC, 2D and SDS electrophoresis.	Mitochondrial proteomics abnormalities, MMP proteins loss, nuclear DNA damage, genotoxic effect. GAPDH inhibition, increased levels of methylglyoxal-associated DNA damage.	[55]
Chicken embryo HHO Neural stem cells Neuroblastoma SH-SY5Y cell	50 nm	Synthesis method ND/OC. TEM, SEM, EDS and DLS	24 h 12 h 12 h	12.5–50 $\mu\text{g}/\text{mL}$ 0–50 $\mu\text{g}/\text{mL}$ 0–50 $\mu\text{g}/\text{mL}$	ND * 25 $\mu\text{g}/\text{mL}$ 25 $\mu\text{g}/\text{mL}$	Cell/embryo IFA, FC, WB, RNA-seq, q-PCR, IFA/FM	Endoplasmic reticulum stress, increased Ca^{2+} levels, Casp-3, increased levels, abnormal mitochondrial morphology. ZnO-NPs induced failure of neural tube closure.	[56]
Neuroblastoma SH-SY5Y cell	24–30 nm	Green synthesis (<i>Clausena lansium</i>) UV-Vis, XRD, FT-IR and TEM	24 h	10–20 $\mu\text{g}/\text{mL}$	15 $\mu\text{g}/\text{mL}$	Cell viability, MTT, ROS levels, WB, CA (DNA damage)	Increased ROS levels, increased levels of BAX, caspase-3, and BCL-2 proteins. Autophagy (beclin-1, LC3-I, LCEII and ATG4B) increased levels. DNA loss and damage. NAC prevents ROS in SH-SY5Y.	[57]
Mouse Leydig cells Mouse Sertoli cells	70 nm	Synthesis method ND/OC. TEM, AFM, XRD, FTIR, UV-Vis, DLS	24 h 24 h	0, 5, 10, 15, and 20 $\mu\text{g}/\text{mL}$	15 $\mu\text{g}/\text{mL}$ 15 $\mu\text{g}/\text{mL}$	MTT, LDH, ROS levels, TUNEL and JC-1 assay, WB, sperm morphology	Increased ROS levels, MMP abnormalities, increased apoptotic proteins, loss of MMP, nuclear DNA damage and breakage.	[58]
Mouse ovarian germ cells (CHO-K1)	80 nm	Co-precipitation method SEM, TEM	24 h (1 day) 168 h (7day)	10, 20 and 30 $\mu\text{g}/\text{mL}$	30 $\mu\text{g}/\text{mL}$ 10 $\mu\text{g}/\text{mL}$	IFA/FM; FC. Quantification of ROS. qRT-PCR of Prdm1, Dppa3, Ifitm3, Ddx4 and Dazl	ROS level, cell membrane integrity. Significant increase in expression of premeiotic germ cells markers but a decrease in meiotic and post-meiotic markers.	[59]
Murine microglial BV-2 cells	20 nm	Synthesised by using the wet chemical method. TEM, SEM, XRD, XPS	6 h 24 h	0–80 $\mu\text{g}/\text{mL}$	20 $\mu\text{g}/\text{mL}$ 10 $\mu\text{g}/\text{mL}$	MTT, TBEA, FC, MMP, ROS levels, PMP levels, cell cycle analysis, WB	Absence of caspase-3 cleavage and PARP fragmentation. Mitochondrial dysfunction and lysosomal alteration increased PMP. Accumulation of ROS. Non-apoptotic hallmarks, necrotic markers in BV-2 cells.	[60]

Table 1. Cont.

Cell Type	Size and Shape of ZnO-NP	Synthesis and Characterization of ZnO-NPs	Time of Exposition (h)	Doses mg/L	IC50	Biological Characterization	Mitochondrial Pathway	Reference
<i>S. Cerevisiae</i> (yeast BY4743)	20–80 nm	Synthesis method ND/OC. SEM, HRFESEM, UV-Vis and DLS analysis.	3 h	5–20 µg/mL	10 µg/mL	Cell death assay. WB, ROS levels, chitin and lipid droplets measurement. Vacuolar organelle morphology. RT-PCR	Mitochondrial morphology and lipid homeostasis abnormalities, ROS elevation. Perturbations in peripheral endoplasmic reticulum. ZnO-NPs do not affect histone epigenetic marks. Increased levels of Hog1. Inhibition of cell growth due alterations in CWI and HOG signaling pathway.	[27]
<i>S. Cerevisiae</i> (yeast BY4741)	20–80 nm	Synthesis method ND/OC. SEM, HRFESEM, UV-Vis	3 h	10 µg/mL	10 µg/mL	Cell culture, WB, HNMR, RT-PCR. RNA and metabolites identification/quantification	Mitochondrial expression of PSD1, SOD1, SOD2, KGD1 TCA cycle genes (ACO1 and KDG1) Oxidative pathway abnormalities (SOD1, SOD2 and YAP1) Lipid biosynthesis pathway abnormalities (INO2, INO4, CHO1, PSD1 and CRD1)	[28]

ND/OC: not determined/obtained commercially; NS *: not significant at the maximum doses of ZnO-NP exposure; TEM: transmission electron microscopy; XRD: x-ray diffraction; MTT: [3-(4,5-dimethylthiazoyl-2-yl)-2,5 e diphenylte-trazolium bromide]; LDH: lactate dehydrogenase; LA: antioxidant alpha-lipoic acid; ROS: reactive oxygen species; FM: fluorescence microscopy; MMP: mitochondrial membrane potential; CACAk: Caspase Apoptosis Colorimetric Assay Kit; Cyt-c: measurements of Cyt-c release; ICC: immunocytochemistry; IFA: immunofluorescence; SEM-EDS: scanning electron microscope-energy dispersive spectroscopy; DLS: Dynamic Light Scattering; CNCCs: primary culture of cranial neural crest cells; ARS: Alizarin red staining; IHC: immunohistochemistry; RNA-seq: RNA sequencing transcript profiling; q-PCR: quantitative polymerase chain reaction; DHE: dihydroethidium staining; HCA: High-Content Analysis; CCK-8: cell viability was analyzed by using the Cell Counting Kit-8; WB: Western Blot; MEA: Microelectrode Assay; RT-CES: real-time cell electronic sensing system; ELISA: enzyme-linked immunosorbent assay; FC: flow cytometry; FSP-1: fibroblast-specific protein-1; Apaf-1: protease-activating factor-1; FTIR: Fourier transform infrared; SOD: superoxide dismutase; CAT: catalase; TBARS: thiobarbituric acid reactive substances; LPO: lipid peroxidation; GST: glutathione-S-transferase; GSH: glutathione estimation; OH: hydroxyl radicals; O2: superoxide radical; UV-Vis: UV-visible spectroscopy; DAPI: 4',6'-diamidino-2 phenylindole; Cas-3: caspase-3; Cas-9: caspase-9; H: hemolysis; MDA: determination of lipid peroxidation; NO: nitric oxide production; IL-6: interleukin 6; TNF- α : tumor necrosis factor α ; HRTEM: high-resolution transmission electron microscopy; FESEM: field-emission scanning electron microscope; VWH: Vitro Wound Healing; CA: Comet Assay; DNAf: DNA Fragmentation; RT-qPCR: Reverse Transcription-Quantitative Polymerase Chain Reaction; FACScan: fluorescence associated cell sorter scan; ZXA: Zebrafish Xenograft Assay; GAPDH: glyceraldehyde 3-phosphate dehydrogenase; MDC: Autophagic Vacuole Indicator Monodansylcadaverine; ICP-AES: inductively coupled plasma atomic emission spectroscopy; AVO: acidic vesicular organelles; ICP-MS: Inductively Coupled Plasma Mass Spectroscopy; SAED: Selected Area Electron Diffraction; AO/EB: acridine orange/ethidium bromide; PI: propidium iodide; HNMR: hydrogen-1 nuclear magnetic resonance spectroscopy; HR-FESEM: high-resolution field-emission scanning electron microscope; CWI: cell wall integrity; TCA: tricarboxylic acid cycle; XPS: X-ray photoelectron spectroscopy; TBEA: trypan blue exclusion assay; PMP: plasma membrane permeability; HPLC: high-performance liquid chromatography; DPPH: 2,2-diphenyl-1-picrylhydrazyl; ABTS: 2,2'-Azino-Bis-3-Ethylbenzothiazoline-6-Sulfonic Acid.

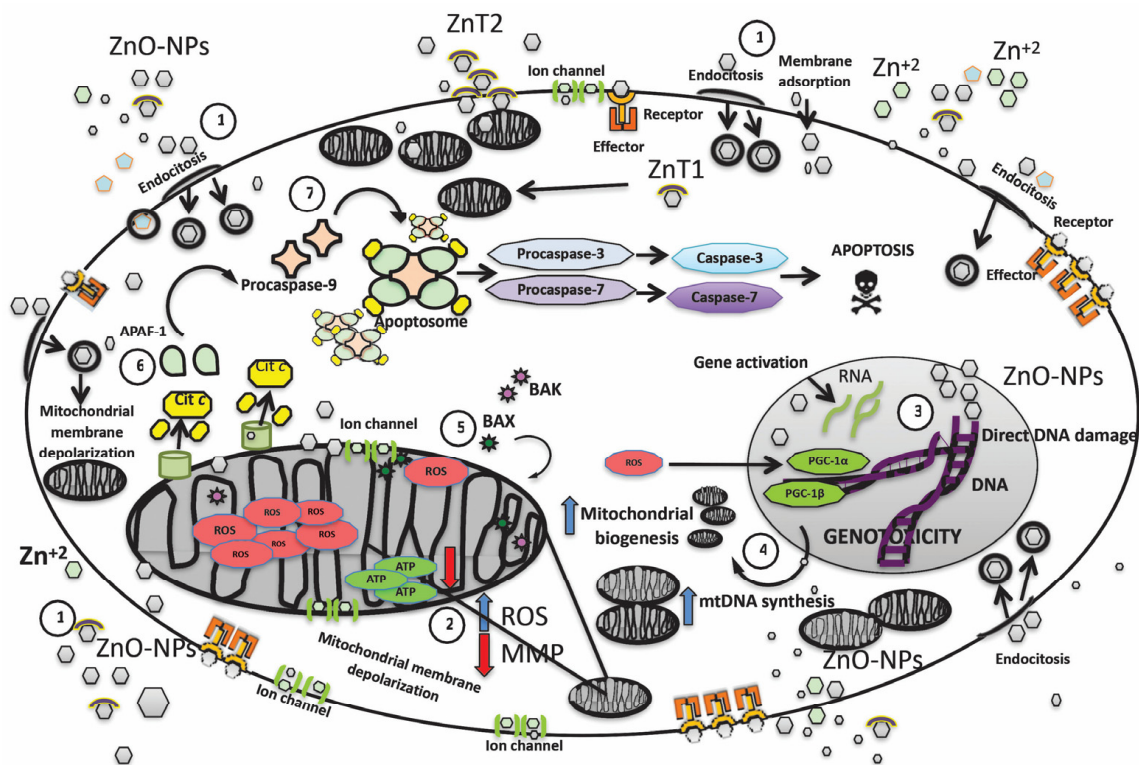


Figure 1. An integrated overview of the molecular pathways activated by ZnO-NP exposure inside the cell, while also summarizing the initial mitochondrial effects such as increased mitochondrial biogenesis, the potential depolarization of the mitochondrial membrane, increased ROS production, and the cumulative effects of ZnO-NPs leading to activation of the intrinsic (mitochondrial) pathway of programmed cell death. 1. ZnO-NPs penetrate the cell membrane via four mechanisms: the first mechanism occurs when ZnO-NPs interact with receptors embedded in the cell membrane, which, in association with the effector, function as second messengers, activating other signaling pathways. The second mechanism occurs when ion channels facilitate entry into the cytoplasm. The third mechanism is endocytosis—in this process, a fragment of the lipid cell membrane covers ZnO-NPs, allowing the formation of vacuoles, which later merge with the membranes of other organelles such as the nucleus and the mitochondria. The fourth mechanism is direct absorption, in which ZnO-NPs (depending on their size and shape) penetrate the cellular lipid bilayer. The entry of ZnO-NPs is also facilitated by two specialized zinc transporters, called ZnT1 and ZnT2. Zinc dissociation also occurs, and zinc can penetrate as zinc ions. The effects of ZnO-NPs depend on the dose, the exposure time, the size of the nanoparticles—as mentioned above, the smaller the size, the greater the cytotoxic effect—and also the shape (spherical, hexagonal, tubular, etc.) [9,10,36] 2. ZnO-NPs, such as Zn ions, readily enter all cellular compartments, including mitochondria, mainly through mitochondrial ion channels, conditioning the voltage change and depolarization of the inner mitochondrial membrane. Within the inner membrane, there is also the protein complex that constitutes the electron transport chain responsible for the synthesis of ATP. ZnO-NPs not only induce a decrease in MMP due to ion channel damage but also cause a decrease in ATP production and an increase in ROS production [13]. 3. The increase in ROS levels in the cell nucleus causes direct damage to the genetic material (double-strand breaks and the oxidation of nitrogenous bases), induces a greater expression of the PGC-1 α and PGC-1 β factors in the nucleus, and promotes mitochondrial biogenesis, to compensate for the increased energy demands [15,16,21] 4. mtDNA replication and transcription pathways are simultaneously activated. mtDNA number is significantly increased in cells exposed to ZnO-NP to counteract mitochondrial oxidative damage under mild oxidative stress [31]. 5. As cellular stress increases, the pathways to compensate for the damage trigger the release of pro-apoptotic proteins, such as BCL-associated protein X-2 (BAX) and/or BCL antagonist/killer-2 (BAK). Activated BAX or BAK

forms pores in the mitochondrial membrane, leading to the release of apoptogenic molecules [34,35,47]. 6. leads to the release of pro-apoptotic proteins, including cytochrome-c and Apaf-1. 7. Finally, pro-caspase-9 is added, to form the apoptosome, which promotes the activation of pro-caspase-3 and pro-caspase-7 and conversion to caspase-3 and caspase-7, respectively; this protein complex will initiate cell dismantling and lead to apoptosis. ROS: reactive oxygen species; MMP: mitochondrial membrane potential; ZnO-NPs: zinc oxide nanoparticles; Cit-c: cytochrome-c; APAF-1: apoptosis protease-activating factor-1; ZnT1, ZnT2: Zinc transporter 1/2; mtDNA: mitochondrial DNA; BAX: BCL-2-associated X protein; BAK: BCL-2 antagonist/killer; PGC-1 α : peroxisome proliferator-activated receptor gamma-coactivator 1 α and 1 β [61–63].

3. Apoptosis Induction ZnO-NPs

To maintain normal tissue function, damaged or aged cells are constantly eliminated by apoptosis. There are two routes to initiate apoptosis: the extrinsic pathway, conditioned by the binding of extracellular factors to the receptors present in the plasma membrane, and the intrinsic pathway, mediated by the action of mitochondrial factors [64]. The intrinsic apoptosis pathway is activated by physical (radiation), chemical (ZnO-NPs), or biological (viruses) stimuli. The BCL-2 family proteins orchestrate the regulation and execution of this pathway, which includes both pro-apoptosis and pro-survival proteins [65]. To initiate apoptosis, cellular stress or damage signals turn on the cascade of pro-apoptotic proteins, such as BCL-2-associated protein X (BAX) and/or BCL-2 antagonist/killer (BAK). Once activated, BAX or BAK induces mitochondrial pore formation. Provoking the release of apoptogenic molecules, which includes the second mitochondria-derived caspase activator (SMAC), serine proteases called caspases, and cytochrome-c derived from the mitochondrial intermembrane space. The mitochondrial release of cytochrome-c into the cytoplasm leads to the formation of apoptosomes. These events promote the activation of the initiator caspase (caspase-9) and executioner caspases (caspases-3, 6, and 7) for the orderly dismantling of the cell [61,62,66]. Considering the complexity of cancer treatment and that ZnO-NPs activate the intrinsic apoptosis pathway and caspases, the study of the cytotoxic response to ZnO-NP exposure in tumor cells is promising. A study performed on gingival squamous cell carcinomas (GSCC) in two human cell lines (Ca9-22 and OECM-1). Showed that ZnO-NPs induced growth inhibition of GSCCs, and did not cause damage to normal human keratinocytes (HaCaT cells) or gingival fibroblasts (HGF-1 cells). ZnO-NPs caused apoptotic death of GSCC cells in a concentration-dependent manner, increased intracellular ROS and specifically superoxide levels. Importantly, antioxidant and caspase inhibitors prevent ZnO-NP-induced cell death, indicating that humans' superoxide-induced mitochondrial dysfunction is related to caspase-mediated apoptosis. On the other hand, treatment of ZnO-NPs in a dose-dependent condition triggered the expression of p53, BAX, and cytochrome-c in ovarian and cervical tumor cells. The expression of caspase-9, caspase-3, cleaved caspase-9 and cleaved caspase-3 in HeLa cells was increased in cells treated with ZnO-NPs, compared with control cells. Multiple experiments in carcinogenic human hepatocytes HepG2 and HL-7702 cells, human hepatocytes cancer Huh7 cells, chronic myelogenous leukemia cells, Human colorectal Caco-2, colon carcinoma HCT116 cells, human cervical cancer SiHa cells and HeLa cells, cell models such as human ovarian cancer SKOV3, and neuroblastoma SH-SY5Y cells, breast cancer MDAMB-23 and MCF-7 cells, human head, and neck squamous cell carcinoma FaDu cells, showed a dose-dependent effect after treatment with ZnO-NPs [38,53,67–69], resulting in stimulation of the intrinsic pathway of apoptosis with very similar patterns.

ZnO-NPs induced similar changes in transcript levels of diverse proteins, such as p53, BAX, BCL-2, CYT-c, CAS-9, CAS-8 and CAS-3, with significant differences versus control cell models. They also documented the induction of apoptosis through oxidative stress-mediated Ca²⁺ release, ROS generation, and loss of mitochondrial membrane potential. Tumor cells have an increased susceptibility to ZnO-NP exposure. ZnO-NPs also induce

apoptosis in germ ovarian germ cells CHO-K1, male germ Leydig and Sertoli cells (mouse model), causing time-dose-dependent damage, genotoxicity caused by increased ROS, and loss of mitochondrial membrane potential was reported. In addition, injection of ZnO-NPs into male mice caused structural alterations in the seminiferous epithelium and sperm abnormalities [58,59]. In 2020, Sruthi et al. [60], proposed a non-apoptotic mode of cell death following exposure of ZnO-NPs in murine microglial BV-2 cells. By triggering an accumulation of ROS favoring altered and increased plasma membrane permeability and also loss of mitochondrial membrane potential, leading to the formation of “ghost cells” without apoptotic features, there was no caspase-3 or PARP fragmentation in BV-2 cells. However, an adaptive response involving increased mitochondrial biogenesis cannot be excluded.

4. Caspases Expression and ZnO-NPs

The caspases are at the core of executing apoptosis by orchestrating cellular destruction with a proteolytic mechanism. Caspases are a family of at least a dozen cysteine proteases; they are expressed as inactive proteases [70–72]. Caspase activation occurs by cleavage of the pro-domain and inter-subunit linker, the latter of which is most critical. The mature enzyme is formed by a dimer containing a small and a large subunit that generates an active site on each side. Apoptotic caspases are functionally subdivided into initiator (caspases-8, 9, and 10) and effector (caspases-3, 6, and 7). Apaf-1 attaches to cytochrome-*c* and procaspase-9 to form a proteic complex called the apoptosome that activates the caspase-3, which finally initiates apoptosis. Because caspase-3 is involved in the final molecular steps, it is used as a molecular marker to confirm apoptosis. It is well documented that mRNA levels of caspase-3, caspase-9, and Apaf-1 increase dose-dependent mode after ZnO-NP exposure. Thus, ZnO-NPs induce caspase signaling-related protein expression. In a study by Cheng et al. in bone cancer cells, there is a substantial increase in the protein levels of BAX, caspase-3 and caspase-9 when treated with ZnO-NPs, compared with control cells. Control cells displayed a decreased rate of apoptosis.

Cells administered with 50 µg/mL of ZnO-NPs exhibited a higher rate of apoptosis than cells supplemented with 30 µg/mL of ZnO-NPs [53,73–75]. Tumor cells show greater susceptibility to apoptosis after exposure to ZnO-NPs. Considering that the molecular changes in cancer cells include resistance to apoptosis, which can lead to immortality and a high rate of cellular division, ZnO-NPs undoubtedly constitute a very promising line of therapeutic research. Pro-apoptotic and anti-apoptotic molecules, such as p53 and the B-cell lymphoma 2 (BCL-2) family, closely regulate apoptosis. ZnO-NPs treatment causes a significant increase in mRNA expression of cell cycle checkpoint proteins p53, BAX, and caspase-3 and downregulates anti-apoptotic BCL-2 proteins in epidermoidal carcinoma cells. A similar effect in the overexpression of p53 was reported in hepatocytes and kidney tissue after oral administration in rats with ZnO-NPs. ROS induces the translocation, phosphorylation, and cleavage of pro-apoptosis BCL-2 members, leading to the induction of apoptosis. Caspase-9 and caspase-3 activation can be completely abolished by the presence of antioxidants, which confirms that is a ROS-dependent pathway in ZnO-NP-induced apoptosis [33,76]. On the other hand, there are reported differences in apoptotic gene expression between fresh and aged ZnO-NPs. Wang et al., in 2020, reported at least a dozen apoptosis genes that were significantly overexpressed in fresh ZnO-NP-exposed cells, compared to only half of the genes overexpressed in human peripheral blood T lymphocyte cells after addition of aged ZnO-NPs; interestingly, the expression of caspase-3 was not significantly changed [77]. ZnO-NPs are used in numerous dermatological products, cosmetics and sunscreens. Application of ZnO to the skin increases the level of zinc ions in the epidermis, then in the systemic circulation, and finally in the urine; although the amount that penetrates the skin and enters the circulation is low, it can be detected in urine and blood. Therefore, in vivo studies on blood cells, including erythrocytes, lymphocytes, monocytes, eosinophils, and platelets, are essential. In a study using 100–130 nm ZnO-NPs, lymphocytes were found to be the most sensitive to the action of the NPs. Human B lym-

phocyte and human monocyte cell lines were the most susceptible to the activity of 100 nm diameter nanoparticles. In contrast, human T lymphocytes and human promyelocytes were slightly more sensitive to 130 nm ZnO-NPs. Human promyelocytes are the most resistant to ZnO nanoparticles, while human monocytes are the most sensitive. When exposed to ZnO-NPs with a diameter of 15–24 nm, human lymphocytes display a dose-dependent decrease in mitochondrial activity. Khan et al., [35] in 2015, found ROS elevation and hemolytic action conditioned by ZnO-NPs in human erythrocytes. In contrast, in human eosinophils, ZnO-NPs delays apoptosis through caspase suppression and de novo protein synthesis. This evidence demonstrates that although caspases are ubiquitous proteins in all multicellular systems, cell type, energetic demands and their functions play an important role and influence susceptibility to apoptosis [35–37,78].

5. Effect of ZnO-NPs in Mitochondrial Membrane Potential

Mitochondrial membrane potential (MMP) maintains efficient ATP synthesis and an appropriate proton gradient across its lipid bilayer; also its integrity plays a vital role in inducing apoptosis. The effects of ZnO-NPs on MMP are widely studied. Pro-apoptosis BCL-2 family proteins also induce the permeabilization of the outer mitochondrial membrane, as well as modulate mitochondrial homeostasis for contributing to the loss of MMP. There is a strong correlation between MMP and ROS production and it is widely accepted that mitochondria produce more ROS at a high membrane potential. Depolarization of MMP produced either by a closure of the mitochondrial permeability transition pore or inhibition of ATP synthase is associated with increased ROS production. Additionally, the mitochondrial permeability transition pore has been demonstrated to induce depolarization of MMP, release of apoptogenic factors and loss of oxidative phosphorylation. Wang et al., in 2018, reported that ZnO-NPs increased the intracellular ROS level and decreased MMP in CAL 27 oral cancer cell lines. Similar results were reported in AGS gastric cancer cells, with significantly reduced MMP levels; this diminution of MMP after inner mitochondrial membrane permeabilization stimulates the release of several apoptotic factors [40,52,78].

6. Conclusions

This systematic review aimed to include the most recent scientific evidence concerning the cytotoxic effect of ZnO-NPs in biological models and in particular on mitochondrial damage in multiple biological models. Since mitochondria are among the most complex and relevant organelles for cellular homeostasis, it is indispensable to define the most relevant mechanisms leading to cell dysfunction/death. Although the applications of ZnO-NPs have revolutionized modern life with unprecedented advances in the medical field, their harmful and cytotoxic effects cannot be neglected. The unique properties of ZnO-NPs are dependent on morphology, size, concentration, and exposition period.

The contribution and usefulness of ZnO-NPs in medical oncology is of great interest; in particular, their contribution in the therapeutic area is increasingly relevant due to the immense potential in the public health sector because cancer remains among the leading causes of death worldwide. Tumor cells show a different cytotoxic effect compared to healthy cells of the same lineage, and the response also varies depending on the exposure time, size and shape of ZnO-NPs. Due to the heterogeneity in research design, more *in vitro* investigations are required, to determine the exact mechanisms of cytotoxicity, and further clarify the anti-cancer effect of ZnO-NPs. Therefore, it is imperative to perform further *in vitro* trials with different tumor lines from the same tissue—for example, the human cervical cancer cell SiHa and the cervical cancer cell line HeLa—at different concentrations to properly examine the cytotoxic properties of ZnO-NPs. More emphasis should be given to the correlation between the size (5–100 nm) and structural shapes, including spherical, oval, elongated, irregular, and hexagonal, of ZnO-NPs and their mitochondrial toxicity. Because ZnO-NPs can act as anti-cancer agents against different tumor lines resistant to conventional chemotherapeutic treatments, they provide a talented substitute approach to chemotherapies.

On the other hand, other important characteristic of ZnO-NPs, with the same impact on public health, are the possible teratogenic effects in embryonic cell models, affecting migration, cell–cell interaction and cell differentiation as well as intervening in mitochondrial pathways, as already mentioned.

Since we are certainly in daily contact with ZnO-NPs, more attention needs to be addressed to them, since bioaccumulation of these elements can occur in plants, food and aquatic species, with a direct impact on human and environmental health. Table 2 aims to summarize the most relevant factors involved in the mitochondrial and cellular response after exposure to ZnO-NPs found in the most relevant literature. We believe that this systematic review provides information on correlation and impact on future research.

Table 2. Effects triggered after exposure to ZnO-NPs.

Mitochondrial Pathway	ZnO-NPs Effect
Mitochondrial biogenesis	<ul style="list-style-type: none"> ↑ mDNA replication and transcription systems. ↑ PSD1 to mitochondrial maintenance. ↑ Mitochondrial biogenesis by PGC-1. ↑ Mitophagy.
Apoptosis induction	<ul style="list-style-type: none"> ↑ p53, BAX, BAK, SMAC and cytochrome-c levels to induce apoptosis. ↑ DNA fragmentation and cytoplasmic reduction. ↑ Anti-BCL2.
Caspases induction	<ul style="list-style-type: none"> ↑ Pro-caspases-9 and pro-caspase-3 to convert in activated caspase-9. ↑ Apaf-1. ↑ Apoptosome.
Mitochondrial membrane potential	<ul style="list-style-type: none"> ↑ Mitochondrial membrane potential. ↑ ATP synthase. ↑ Reactive oxygen species. ↑ Mitochondrial pore abnormalities with delivery of pro-apoptotic proteins.

↑: Increase; mDNA: mitochondrial DNA; PSD1: phosphatidylserine decarboxylase 1; PGC-1: peroxisome proliferator-activated receptor γ coactivator 1 α ; p53: p53 protein; BAX; Bax protein; BAK: Bak protein; SMAC: second mitochondria-derived activator of caspase; BCL2: B-cell lymphoma-2 proteins; Apaf-1: Apoptotic Peptidase-Activating Factor 1; ATP synthase: adenosine triphosphate synthase.

Author Contributions: L.P.-R., V.L.-C., I.L.-A., M.Á.L.-Á., J.A.A.-P. and I.P.-L. gathered the research data. L.P.-R., P.A.L.-M. and H.A.-R. analyzed these data and wrote this review paper. All authors have read and agreed to the published version of the manuscript.

Funding: This research received no external funding.

Institutional Review Board Statement: Not applicable.

Informed Consent Statement: Not applicable.

Data Availability Statement: All data is in this review.

Conflicts of Interest: The authors declare no conflict of interest.

References

- Mathew, E.N.; Hurst, M.N.; Wang, B.; Murthy, V.; Zhang, Y.; De Long, R.K. Interaction of Ras Binding Domain (RBD) by chemotherapeutic zinc oxide nanoparticles: Progress towards RAS pathway protein interference. *PLoS ONE* **2020**, *15*. [[CrossRef](#)] [[PubMed](#)]
- Bharathi, D.; Bhuvaneshwari, V. Synthesis of zinc oxide nanoparticles (ZnO NPs) using pure bioflavonoid rutin and their biomedical applications: Antibacterial, antioxidant and cytotoxic activities. *Res. Chem. Intermed.* **2019**, *45*, 2065–2078. [[CrossRef](#)]
- Danielsen, P.H.; Cao, Y.; Roursgaard, M.; Møller, P.; Loft, S. Endothelial cell activation, oxidative stress and inflammation induced by a panel of metal-based nanomaterials. *Nanotoxicology* **2015**, *9*, 813–824. [[CrossRef](#)] [[PubMed](#)]
- Liu, N.; Tang, M. Toxic effects and involved molecular pathways of nanoparticles on cells and subcellular organelles. *J. Appl. Toxicol.* **2020**, *40*, 16–36. [[CrossRef](#)]

5. Hu, X.; Cook, S.; Wang, P.; Hwang, H.-M. In vitro evaluation of cytotoxicity of engineered metal oxide nanoparticles. *Sci. Total Environ.* **2009**, *407*, 3070–3072. [[CrossRef](#)] [[PubMed](#)]
6. Sharma, V.; Shukla, R.K.; Saxena, N.; Parmar, D.; Das, M.; Dhawan, A. DNA damaging potential of zinc oxide nanoparticles in human epidermal cells. *Toxicol. Lett.* **2009**, *185*, 211–218. [[CrossRef](#)] [[PubMed](#)]
7. Donaldson, K.; Stone, V.; Clouter, A.; Renwick, L.; Macnee, W. Ultrafine particles. *Occup. Environ. Med.* **2001**, *58*, 211–216. [[CrossRef](#)] [[PubMed](#)]
8. Yan, Y.; Wang, G.; Huang, J.; Zhang, Y.; Cheng, X.; Chuai, M.; Brand-Saberi, B.; Chen, G.; Jiang, X.; Yang, X. Zinc oxide nanoparticles exposure-induced oxidative stress restricts cranial neural crest development during chicken embryogenesis. *Ecotoxicol. Environ. Saf.* **2020**, *194*, 110415. [[CrossRef](#)] [[PubMed](#)]
9. Wang, M.; Wang, J.; Liu, Y.; Wang, J.; Nie, Y.; Si, B.; Liu, Y.; Wang, X.; Chen, S.; Hei, T.K.; et al. Subcellular Targets of Zinc Oxide Nanoparticles during the Aging Process: Role of Cross-Talk between Mitochondrial Dysfunction and Endoplasmic Reticulum Stress in the Genotoxic Response. *Toxicol. Sci.* **2019**, *171*, 159–171. [[CrossRef](#)]
10. Limo, M.J.; Sola-Rabada, A.; Boix, E.; Thota, V.; Westcott, Z.C.; Puddu, V.; Perry, C.C. Interactions between Metal Oxides and Biomolecules: From Fundamental Understanding to Applications. *Chem. Rev.* **2018**, *118*, 11118–11193. [[CrossRef](#)] [[PubMed](#)]
11. Popov, L.D. Mitochondrial biogenesis: An update. *J. Cell. Mol. Med.* **2020**, *24*, 4892–4899. [[CrossRef](#)] [[PubMed](#)]
12. Zhao, L.; Sumberaz, P. Mitochondrial DNA Damage: Prevalence, Biological Consequence, and Emerging Pathways. *Chem. Res. Toxicol.* **2020**, *33*, 2491–2502. [[CrossRef](#)] [[PubMed](#)]
13. Yu, S.B.; Pekkurnaz, G. Mechanisms Orchestrating Mitochondrial Dynamics for Energy Homeostasis. *J. Mol. Biol.* **2018**, *430*, 3922–3941. [[CrossRef](#)] [[PubMed](#)]
14. Wang, F.; Zhang, D.; Zhang, D.; Li, P.; Gao, Y. Mitochondrial Protein Translation: Emerging Roles and Clinical Significance in Disease. *Front. Cell Dev. Biol.* **2021**, *9*, 675465. [[CrossRef](#)] [[PubMed](#)]
15. Yokokawa, T.; Kido, K.; Suga, T.; Isaka, T.; Hayashi, T.; Fujita, S. Exercise-induced mitochondrial biogenesis coincides with the expression of mitochondrial translation factors in murine skeletal muscle. *Physiol. Rep.* **2018**, *6*, e13893. [[CrossRef](#)]
16. Holt, A.G.; Davies, A.M. The significance of mitochondrial DNA half-life to the lifespan of post-mitotic cells. *bioRxiv* **2020**. [[CrossRef](#)]
17. Byrne, J.J.; Soh, M.S.; Chandhok, G.; Vijayaraghavan, T.; Teoh, J.S.; Crawford, S.; Cobham, A.E.; Yapa, N.M.B.; Mirth, C.K.; Neumann, B. Disruption of mitochondrial dynamics affects behaviour and lifespan in *Caenorhabditis elegans*. *Cell. Mol. Life Sci.* **2019**, *76*, 1967–1985. [[CrossRef](#)]
18. Yu, R.; Lendahl, U.; Nistér, M.; Zhao, J. Regulation of Mammalian Mitochondrial Dynamics: Opportunities and Challenges. *Front. Endocrinol.* **2020**, *11*, 374. [[CrossRef](#)]
19. Zhang, C.S.; Lin, S.C. AMPK promotes autophagy by facilitating mitochondrial fission. *Cell Metab.* **2016**, *23*, 399–401. [[CrossRef](#)]
20. Wu, Z.; Puigserver, P.; Andersson, U.; Zhang, C.; Adelmant, G.; Mootha, V.; Troy, A.; Cinti, S.; Lowell, B.; Scarpulla, R.C.; et al. Mechanisms controlling mitochondrial biogenesis and respiration through the thermogenic coactivator PGC-1. *Cell* **1999**, *98*, 115–124. [[CrossRef](#)]
21. Gureev, A.P.; Shaforostova, E.A.; Popov, V.N. Regulation of mitochondrial biogenesis as a way for active longevity: Interaction between the Nrf2 and PGC-1 α signaling pathways. *Front. Genet.* **2019**, *10*, 435. [[CrossRef](#)] [[PubMed](#)]
22. Li, Y.; Li, F.; Zhang, L.; Zhang, C.; Peng, H.; Lan, F.; Peng, S.; Liu, C.; Guo, J. Zinc oxide nanoparticles induce mitochondrial biogenesis impairment and cardiac dysfunction in human ipsc-derived cardiomyocytes. *Int. J. Nanomed.* **2020**, *15*, 2669–2683. [[CrossRef](#)] [[PubMed](#)]
23. Yousef, M.I.; Mutar, T.F.; Kamel, M.A.E.N. Hepato-renal toxicity of oral sub-chronic exposure to aluminum oxide and/or zinc oxide nanoparticles in rats. *Toxicol. Rep.* **2019**, *6*, 336–346. [[CrossRef](#)] [[PubMed](#)]
24. Liu, Y.J.; McIntyre, R.L.; Janssens, G.E.; Houtkooper, R.H. Mitochondrial fission and fusion: A dynamic role in aging and potential target for age-related disease. *Mech. Ageing Dev.* **2020**, *186*, 111212. [[CrossRef](#)]
25. Li, J.; Zhang, B.; Chang, X.; Gan, J.; Li, W.; Niu, S.; Kong, L.; Wu, T.; Zhang, T.; Tang, M.; et al. Silver nanoparticles modulate mitochondrial dynamics and biogenesis in HepG2 cells. *Environ. Pollut.* **2020**, *256*, 113430. [[CrossRef](#)] [[PubMed](#)]
26. Aung, L.H.H.; Jumbo, J.C.C.; Wang, Y.; Li, P. Therapeutic potential and recent advances on targeting mitochondrial dynamics in cardiac hypertrophy: A concise review. *Mol. Ther. Nucleic Acids* **2021**, *25*, 416–443. [[CrossRef](#)]
27. Babele, P.K.; Thakre, P.K.; Kumawat, R.; Tomar, R.S. Zinc oxide nanoparticles induce toxicity by affecting cell wall integrity pathway, mitochondrial function and lipid homeostasis in *Saccharomyces cerevisiae*. *Chemosphere* **2018**, *213*, 65–75. [[CrossRef](#)]
28. Kumar Babele, P. Zinc oxide nanoparticles impose metabolic toxicity by de-regulating proteome and metabolome in *Saccharomyces cerevisiae*. *Toxicol. Rep.* **2019**, *6*, 64–73. [[CrossRef](#)] [[PubMed](#)]
29. Bird, A.J.; Wilson, S. Zinc homeostasis in the secretory pathway in yeast. *Curr. Opin. Chem. Biol.* **2020**, *55*, 145–150. [[CrossRef](#)] [[PubMed](#)]
30. Chevallet, M.; Gallet, B.; Fuchs, A.; Jouneau, P.H.; Um, K.; Mintz, E.; Michaud-Soret, I. Metal homeostasis disruption and mitochondrial dysfunction in hepatocytes exposed to sub-toxic doses of zinc oxide nanoparticles. *Nanoscale* **2016**, *8*, 18495–18506. [[CrossRef](#)]
31. Yu, K.N.; Yoon, T.J.; Minai-Tehrani, A.; Kim, J.E.; Park, S.J.; Jeong, M.S.; Ha, S.W.; Lee, J.K.; Kim, J.S.; Cho, M.H. Zinc oxide nanoparticle induced autophagic cell death and mitochondrial damage via reactive oxygen species generation. *Toxicol. Vitro* **2013**, *27*, 1187–1195. [[CrossRef](#)] [[PubMed](#)]

32. Khan, M.F.; Siddiqui, S.; Zia, Q.; Ahmad, E.; Jafri, A.; Arshad, M.; Jamal, A.; Alam, M.M.; Banawas, S.; Alshehri, B.A.; et al. Characterization and in vitro cytotoxic assessment of zinc oxide nano-particles in human epidermoid carcinoma cells. *J. Environ. Chem. Eng.* **2021**, *9*, 105636. [[CrossRef](#)]
33. Liang, S.; Sun, K.; Wang, Y.; Dong, S.; Wang, C.; Liu, L.X.; Wu, Y.H. Role of Cyt-C/caspases-9,3, Bax/Bcl-2 and the FAS death receptor pathway in apoptosis induced by zinc oxide nanoparticles in human aortic endothelial cells and the protective effect by alpha-lipoic acid. *Chem. Biol. Interact.* **2016**, *258*, 40–51. [[CrossRef](#)] [[PubMed](#)]
34. Wang, L.; Guo, D.; Wang, Z.; Yin, X.; Wei, H.; Hu, W.; Chen, R.; Chen, C. Zinc oxide nanoparticles induce human tenon fibroblast apoptosis through reactive oxygen species and caspase signaling pathway. *Arch. Biochem. Biophys.* **2020**, *683*, 108324. [[CrossRef](#)] [[PubMed](#)]
35. Khan, M.; Naqvi, A.H.; Ahmad, M. Comparative study of the cytotoxic and genotoxic potentials of zinc oxide and titanium dioxide nanoparticles. *Toxicol. Rep.* **2015**, *2*, 765–774. [[CrossRef](#)]
36. Czyżowska, A.; Dyba, B.; Rudolphi-Szydło, E.; Barbasz, A. Structural and biochemical modifications of model and native membranes of human immune cells in response to the action of zinc oxide nanoparticles. *J. Appl. Toxicol.* **2021**, *41*, 458–469. [[CrossRef](#)] [[PubMed](#)]
37. Czyżowska, A.; Barbasz, A. Cytotoxicity of zinc oxide nanoparticles to innate and adaptive human immune cells. *J. Appl. Toxicol.* **2021**, *41*, 1425–1437. [[CrossRef](#)] [[PubMed](#)]
38. Ahlam, A.A.; Shaniba, V.S.; Jayasree, P.R.; Manish Kumar, P.R. *Spondias pinnata* (L.f.) Kurz Leaf Extract Derived Zinc Oxide Nanoparticles Induce Dual Modes of Apoptotic-Necrotic Death in HCT 116 and K562 Cells. *Biol. Trace Elem. Res.* **2021**, *199*, 1778–1801. [[CrossRef](#)]
39. Wang, S.W.; Lee, C.H.; Lin, M.S.; Chi, C.W.; Chen, Y.J.; Wang, G.S.; Liao, K.W.; Chiu, L.P.; Wu, S.H.; Huang, D.M.; et al. ZnO nanoparticles induced caspase-dependent apoptosis in gingival squamous cell carcinoma through mitochondrial dysfunction and p70s6K signaling pathway. *Int. J. Mol. Sci.* **2020**, *21*, 1612. [[CrossRef](#)]
40. Wang, J.; Gao, S.; Wang, S.; Xu, Z.; Wei, L. Zinc oxide nanoparticles induce toxicity in CAL 27 oral cancer cell lines by activating PINK1/Parkin-mediated mitophagy. *Int. J. Nanomed.* **2018**, *13*, 3441–3450. [[CrossRef](#)]
41. Li, J.; Song, Y.; Vogt, R.D.; Liu, Y.; Luo, J.; Li, T. Bioavailability and cytotoxicity of Cerium- (IV), Copper- (II), and Zinc oxide nanoparticles to human intestinal and liver cells through food. *Sci. Total Environ.* **2020**, *702*, 134700. [[CrossRef](#)] [[PubMed](#)]
42. Ananthalakshmi, R.; Rathinam, S.R.X.R.; Sadiq, A.M. Apoptotic Signalling of Huh7 Cancer Cells by Biofabricated Zinc Oxide Nanoparticles. *J. Inorg. Organomet. Polym. Mater.* **2021**, *31*, 1764–1773. [[CrossRef](#)]
43. Wahab, R.; Siddiqui, M.A.; Saquib, Q.; Dwivedi, S.; Ahmad, J.; Musarrat, J.; Al-Khedhairi, A.A.; Shin, H.S. ZnO nanoparticles induced oxidative stress and apoptosis in HepG2 and MCF-7 cancer cells and their antibacterial activity. *Colloids Surfaces B Biointerfaces* **2014**, *117*, 267–276. [[CrossRef](#)] [[PubMed](#)]
44. Arasu, M.V.; Madankumar, A.; Theerthagiri, J.; Salla, S.; Prabu, S.; Kim, H.S.; Al-Dhabi, N.A.; Arokiyaraj, S.; Duraipandiyan, V. Synthesis and characterization of ZnO nanoflakes anchored carbon nanoplates for antioxidant and anticancer activity in MCF7 cell lines. *Mater. Sci. Eng. C* **2019**, *102*, 536–540. [[CrossRef](#)] [[PubMed](#)]
45. Akhtar, M.J.; Alhadlaq, H.A.; Alshamsan, A.; Majeed Khan, M.A.; Ahamed, M. Aluminum doping tunes band gap energy level as well as oxidative stress-mediated cytotoxicity of ZnO nanoparticles in MCF-7 cells. *Sci. Rep.* **2015**, *5*, 13876. [[CrossRef](#)] [[PubMed](#)]
46. Farasat, M.; Niazvand, F.; Khorsandi, L. Zinc oxide nanoparticles induce necroptosis and inhibit autophagy in MCF-7 human breast cancer cells. *Biologia* **2020**, *75*, 161–174. [[CrossRef](#)]
47. Li, Z.; Guo, D.; Yin, X.; Ding, S.; Shen, M.; Zhang, R.; Wang, Y.; Xu, R. Zinc oxide nanoparticles induce human multiple myeloma cell death via reactive oxygen species and Cyt-C/Apaf-1/Caspase-9/Caspase-3 signaling pathway in vitro. *Biomed. Pharmacother.* **2020**, *122*, 109712. [[CrossRef](#)] [[PubMed](#)]
48. Gowdhami, B.; Jaabir, M.; Archunan, G.; Suganthi, N. Anticancer potential of zinc oxide nanoparticles against cervical carcinoma cells synthesized via biogenic route using aqueous extract of *Gracilaria edulis*. *Mater. Sci. Eng. C* **2019**, *103*, 109840. [[CrossRef](#)]
49. Chen, H.; Luo, L.; Fan, S.; Xiong, Y.; Ling, Y.; Peng, S. Zinc oxide nanoparticles synthesized from *Aspergillus terreus* induces oxidative stress-mediated apoptosis through modulating apoptotic proteins in human cervical cancer HeLa cells. *J. Pharm. Pharmacol.* **2021**, *73*, 221–232. [[CrossRef](#)]
50. Dulta, K.; Koşarsoy Ağçeli, G.; Chauhan, P.; Jasrotia, R.; Chauhan, P.K. A Novel Approach of Synthesis Zinc Oxide Nanoparticles by *Bergenia ciliata* Rhizome Extract: Antibacterial and Anticancer Potential. *J. Inorg. Organomet. Polym. Mater.* **2021**, *31*, 180–190. [[CrossRef](#)]
51. Bai, D.P.; Zhang, X.F.; Zhang, G.L.; Huang, Y.F.; Gurunathan, S. Zinc oxide nanoparticles induce apoptosis and autophagy in human ovarian cancer cells. *Int. J. Nanomed.* **2017**, *12*, 6521–6535. [[CrossRef](#)]
52. Tang, Q.; Xia, H.; Liang, W.; Huo, X.; Wei, X. Synthesis and characterization of zinc oxide nanoparticles from *Morus nigra* and its anticancer activity of AGS gastric cancer cells. *J. Photochem. Photobiol. B Biol.* **2020**, *202*, 111698. [[CrossRef](#)] [[PubMed](#)]
53. Cheng, J.; Wang, X.; Qiu, L.; Li, Y.; Marraiki, N.; Elgorban, A.M.; Xue, L. Green synthesized zinc oxide nanoparticles regulates the apoptotic expression in bone cancer cells MG-63 cells. *J. Photochem. Photobiol. B Biol.* **2020**, *202*, 111644. [[CrossRef](#)] [[PubMed](#)]
54. Patrón-Romero, L.; Luque, P.A.; Soto-Robles, C.A.; Nava, O.; Vilchis-Nestor, A.R.; Barajas-Carrillo, V.W.; Martínez-Ramírez, C.E.; Chávez Méndez, J.R.; Alvelais Palacios, J.A.; Leal Ávila, M.; et al. Synthesis, characterization and cytotoxicity of zinc oxide nanoparticles by green synthesis method. *J. Drug Deliv. Sci. Technol.* **2020**, *60*, 101925. [[CrossRef](#)]

55. Aude-Garcia, C.; Dalzon, B.; Ravanat, J.L.; Collin-Faure, V.; Diemer, H.; Strub, J.M.; Cianferani, S.; Van Dorsselaer, A.; Carrière, M.; Rabilloud, T. A combined proteomic and targeted analysis unravels new toxic mechanisms for zinc oxide nanoparticles in macrophages. *J. Proteomics* **2016**, *134*, 174–185. [[CrossRef](#)]
56. Yan, Y.; Wang, G.; Luo, X.; Zhang, P.; Peng, S.; Cheng, X.; Wang, M.; Yang, X. Endoplasmic reticulum stress-related calcium imbalance plays an important role on Zinc oxide nanoparticles-induced failure of neural tube closure during embryogenesis. *Environ. Int.* **2021**, *152*, 106495. [[CrossRef](#)] [[PubMed](#)]
57. Li, F.; Song, L.; Yang, X.; Huang, Z.; Mou, X.; Syed, A.; Bahkali, A.H.; Zheng, L. Anticancer and genotoxicity effect of (*Clausena lansium* (Lour.) Skeels) Peel ZnONPs on neuroblastoma (SH-SY5Y) cells through the modulation of autophagy mechanism. *J. Photochem. Photobiol. B Biol.* **2020**, *203*, 111748. [[CrossRef](#)]
58. Han, Z.; Yan, Q.; Ge, W.; Liu, Z.G.; Gurunathan, S.; De Felici, M.; Shen, W.; Zhang, X.F. Cytotoxic effects of ZnO nanoparticles on mouse testicular cells. *Int. J. Nanomed.* **2016**, *11*, 5187–5203. [[CrossRef](#)]
59. Saber, M.; Hayaei-Tehrani, R.S.; Mokhtari, S.; Hoorzad, P.; Esfandiari, F. In vitro cytotoxicity of zinc oxide nanoparticles in mouse ovarian germ cells. *Toxicol. Vitro.* **2021**, *70*, 105032. [[CrossRef](#)]
60. Sruthi, S.; Nury, T.; Millot, N.; Lizard, G. Evidence of a non-apoptotic mode of cell death in microglial BV-2 cells exposed to different concentrations of zinc oxide nanoparticles. *Environ. Sci. Pollut. Res.* **2021**, *28*, 12500–12520. [[CrossRef](#)]
61. Singh, R.; Letai, A.; Sarosiek, K. Regulation of apoptosis in health and disease: The balancing act of BCL-2 family proteins. *Nat. Rev. Mol. Cell Biol.* **2019**, *20*, 175–193. [[CrossRef](#)] [[PubMed](#)]
62. Ladokhin, A.S. Regulation of Apoptosis by the Bcl-2 Family of Proteins: Field on a Brink. *Cells* **2020**, *9*, 2121. [[CrossRef](#)] [[PubMed](#)]
63. Morrish, E.; Brumatti, G.; Silke, J. Future Therapeutic Directions for Smac-Mimetics. *Cells* **2020**, *9*, 406. [[CrossRef](#)] [[PubMed](#)]
64. Carneiro, B.A.; El-Deiry, W.S. Targeting apoptosis in cancer therapy. *Nat. Rev. Clin. Oncol.* **2020**, *17*, 395–417. [[CrossRef](#)]
65. Wanner, E.; Thoppil, H.; Riabowol, K. Senescence and Apoptosis: Architects of Mammalian Development. *Front. Cell Dev. Biol.* **2021**, *8*, 1–16. [[CrossRef](#)] [[PubMed](#)]
66. Rajashekara, S.; Shrivastava, A.; Sumhitha, S.; Kumari, S. Biomedical Applications of Biogenic Zinc Oxide Nanoparticles Manufactured from Leaf Extracts of *Calotropis gigantea* (L.) Dryand. *Bionanoscience* **2020**, *10*, 654–671. [[CrossRef](#)]
67. Shobha, N.; Nanda, N.; Giresha, A.S.; Manjappa, P.; Sophiya, P.; Dharmappa, K.K.; Nagabhusana, B.M. Synthesis and characterization of Zinc oxide nanoparticles utilizing seed source of *Ricinus communis* and study of its antioxidant, antifungal and anticancer activity. *Mater. Sci. Eng. C* **2019**, *97*, 842–850. [[CrossRef](#)]
68. Moratin, H.; Scherzad, A.; Gehrke, T.; Ickrath, P.; Radeloff, K.; Kleinsasser, N.; Hackenberg, S. Toxicological characterization of ZnO nanoparticles in malignant and non-malignant cells. *Environ. Mol. Mutagen.* **2018**, *59*, 247–259. [[CrossRef](#)] [[PubMed](#)]
69. Julien, O.; Wells, J.A. Caspases and their substrates. *Cell Death Differ.* **2017**, *24*, 1380–1389. [[CrossRef](#)] [[PubMed](#)]
70. Boice, A.; Bouchier-Hayes, L. Targeting apoptotic caspases in cancer. *Biochim. Biophys. Acta Mol. Cell Res.* **2020**, *1867*, 118688. [[CrossRef](#)] [[PubMed](#)]
71. Nakajima, Y.I.; Kuranaga, E. Caspase-dependent non-apoptotic processes in development. *Cell Death Differ.* **2017**, *24*, 1422–1430. [[CrossRef](#)] [[PubMed](#)]
72. McComb, S.; Chan, P.K.; Guinot, A.; Hartmannsdottir, H.; Jenni, S.; Dobay, M.P.; Bourquin, J.P.; Bornhauser, B.C. Efficient apoptosis requires feedback amplification of upstream apoptotic signals by effector caspase-3 or -7. *Sci. Adv.* **2019**, *5*, 1–12. [[CrossRef](#)]
73. Kopeina, G.S.; Prokhorova, E.A.; Lavrik, I.N.; Zhivotovsky, B. Alterations in the nucleocytoplasmic transport in apoptosis: Caspases lead the way. *Cell Prolif.* **2018**, *51*, e12467. [[CrossRef](#)] [[PubMed](#)]
74. Shalini, S.; Dorstyn, L.; Dawar, S.; Kumar, S. Old, new and emerging functions of caspases. *Cell Death Differ.* **2015**, *22*, 526–539. [[CrossRef](#)] [[PubMed](#)]
75. Giordo, R.; Nasrallah, G.K.; Al-Jamal, O.; Paliogiannis, P.; Pintus, G. Resveratrol inhibits oxidative stress and prevents mitochondrial damage induced by zinc oxide nanoparticles in zebrafish (*Danio rerio*). *Int. J. Mol. Sci.* **2020**, *21*, 3838. [[CrossRef](#)] [[PubMed](#)]
76. Wang, J.; Wang, L. Aged Zinc Oxide Nanoparticles Did Not Induce Cytotoxicity Through Apoptosis Signaling Pathway as Fresh NPs. *Res. Sq.* **2020**. [[CrossRef](#)]
77. Van Opdenbosch, N.; Lamkanfi, M. Caspases in Cell Death, Inflammation, and Disease. *Immunity* **2019**, *50*, 1352–1364. [[CrossRef](#)]
78. Suski, J.; Lebiecinska, M.; Bonora, M.; Pinton, P.; Duszynski, J.; Wieckowski, M.R. Relation between mitochondrial membrane potential and ROS formation. In *Methods in Molecular Biology*; Humana Press Inc.: Totowa, NJ, USA, 2018; Volume 1782, pp. 357–381.